PIER Lighting Research Program

California Energy Commission
Contract # 500-01-041

Draft Photosensor Characterization Report

Deliverable 3.3.1c

February 28, 2003

Submitted To:
Accounting Office, MS-2
California Energy Commission
1516 Ninth Street, 1st Floor
Sacramento, CA 95814

Submitted By:
Architectural Energy Corporation
2540 Frontier Avenue, Suite 201
Boulder, Colorado 80301

Table of Contents

Contact Information:

Subcontract Project Manager
Doug Paton
The Watt Stopper
2800 De La Cruz Blvd.
Santa Clara, CA 95050
(925)-454-8224 voice
(925)-243-8912 fax
Doug_Paton@WattStopper.com

AEC Program Director
Judie Porter
Architectural Energy Corporation
2540 Frontier Avenue
Boulder, CO 80301
303-444-4149 – Voice
303-444-4304 - Fax
jporter@archenergy.com

Prepared By:

Francis Rubinstein, Building Technologies Department, Lawrence Berkeley National Laboratory
Mehry Yazdanian, Building Technologies Department, Lawrence Berkeley National Laboratory
Jim Galvin, Building Technologies Department, Lawrence Berkeley National Laboratory

Project Team
Dr. Richard G. Mistrick, Associate Professor of Architectural Engineering, Pennsylvania State University
Dorene Maniccia, Manager, Market Segment Development, The Watt Stopper

This work was completed under contract to Lawrence Berkeley National Laboratory as part of the California Energy Commission's Lighting Research Program. This program is supported by the California Energy Commission's Public Interest Energy Research (PIER) Buildings Program and the Assistant Secretary for Energy Efficiency and Renewable Energy, Office of Building Technology, Building Technologies Program, of the U.S. Department of Energy under Contract No. DE-AC03-76SF00098.

EXECUTIVE SUMMARY

The report presents the results of laboratory measurements performed on The Watt Stopper's LS-201 photosensor at the Lawrence Berkeley National Laboratory in January 2003. The purpose of these measurements was to characterize the spatial and spectral response function of the LS-201 photosensor. Sample results of the spectral response and spatial response are shown below.

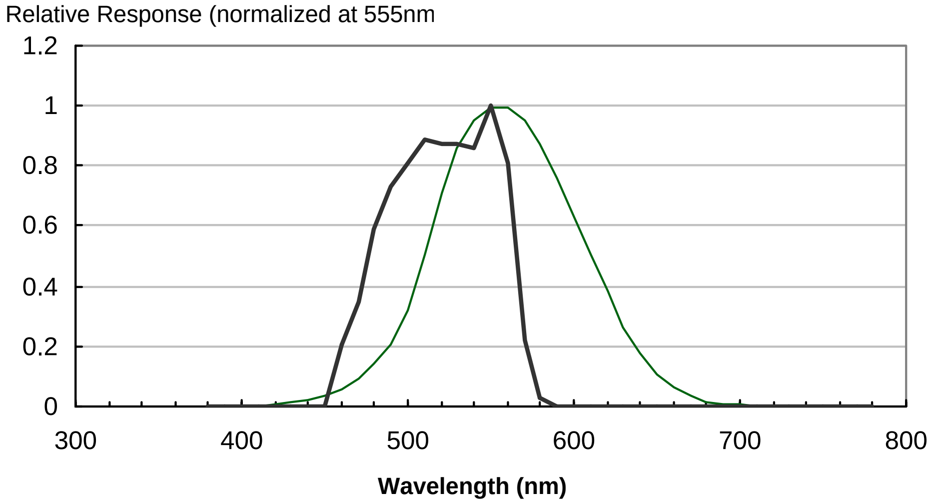

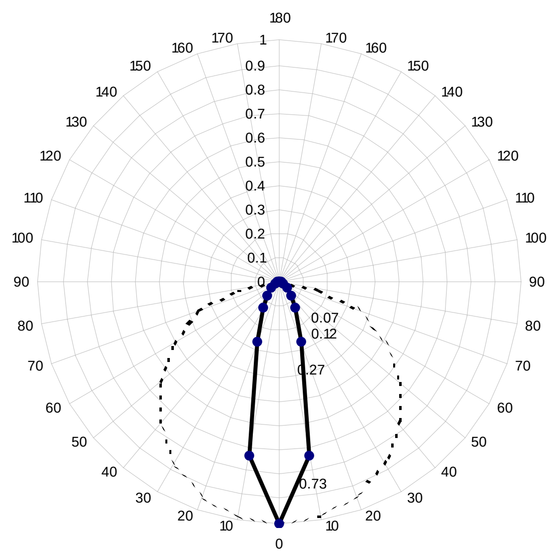

List of Tables

List of Figures

Introduction

This report presents the results of laboratory measurements performed on The Watt Stopper's LS-201 photosensor at the Lawrence Berkeley National Laboratory in January, 2003. The purpose of these measurements was to characterize the spatial and spectral response function of the LS-201 photosensor. This work was performed in fulfillment of a Project 3.3 Deliverable for the California Energy Commission's Lighting Research Program.

The report has three sections. The first section describes the measurements performed to determine the spectral response function (sensitivity to light of different wavelengths) of the photosensor. The second section presents the results of our measurements of the sensitivity of the photosensor to light from different directions – the spatial response function. The third section presents our conclusions and preliminary suggestions for product improvement consistent with project goals and objectives

Characterizing the Spectral Response

The performance of any control photosensor depends on many variables, including its ability to measure the spectral composition of the light within the space in a similar manner as the human eye. The spectral response of a photosensor is expressed as photosensor sensitivity as a function of wavelength of the incident radiation. Previous work has shown that large mismatches between the spectral response of the photosensor and the human eye (as given by the photopic function) can cause significant errors in daylighting control systems. Once the spectral response function of a photosensor has been measured, it is straightforward to compute potential errors in system response solely from knowledge of the spectral composition of the light in the space (fluorescent, daylight, etc).

In Project 3.3, the LBNL Lighting Lab is assisting The Watt Stopper by measuring the spectral response function of candidate photosensors. Since the LS-201 photosensor is the point of departure for subsequent improved designs, we measured the spectral response of this photocell. The purpose of these measurements were to characterize the spectral performance of the photosensor by measuring the spectral response of the photosensor to incident light.

Method

The spectral response of the photosensor was measured by exposing the photosensor to known amounts of monochromic radiation, and measuring the resulting photocell voltage. We used an Ebert monochromator (model JA 82-000), equipped with a 1200 groove per mm grating, to produce quasi-monochromatic radiation from a broadband light source. Figures 1 and 2 show the theory and the design of the Ebert monochromator. Light from a microscope illuminator was focused onto an input 1 mm slit (Figures 3 and

4). The light passing through this slit, was collimated by a concave mirror, which also reflected it onto a diffraction grating. The grating, in turn, directed the light onto a second concave mirror, which reflected and focused it onto an exit slit. Mirrors were used rather than lenses because they do not introduce any chromatic aberration. Because the redirection of the light beam by the grating is actually a diffraction rather than an ordinary reflection, the grating disperses the beam, i.e. different wavelengths leave the grating at different angles. By manually rotating the grating about its central axis, we varied the range of wavelengths, which reflected and focused by the second mirror onto the exit slit. The sensor was placed in front of the exit slit (Figure 4). The output of the photosensor was connected to a voltmeter. The maximum output range for our instrument was from 370 to 750 nanometers. However, due to low system throughput and low sensitivity of the photosensor, the practical range for the sensors we measured was from 440 to 610 nanometers, starting at 610 nm and going down to 440nm. Beyond this range, we did not notice any change in the readings.

We measured the spectral response of two LS201, with and without the lens. These photosensors had been modified by The Watt Stopper for the test so that the photosensors acted like meters (rather than as active control photosensors which would make accurate readings of the response impossible). To measure the actual throughput of the monochrometer, we replaced the photosensor with a silicon-based irradiance probe (Tektronix J6502A) with a known flat response function over the visible range. For this measurement, we replaced the sensor with the photometer. All measurements were taken at 10-nm increments. For all the measurements, we placed the sensor as close as possible to the exit slit, covered the sensor, and turned off the overhead room lights.

Results of the Spectral Response Testing

For this report, we only included the results for one sensor because the test set-up for the second sensor was inadvertently jarred during measurement resulting in artifact that could not be corrected without redoing the measurement. The tabulated data results are summarized in Table 1 and key spectral characteristics given in Figures 5, 6, and 7. Table 1 lists the results of the sensor response, with and without lens, and the output of the monochromator. We corrected the sensor measurements for the offset by subtracting the sensor measurement at the starting point (640 nm) from each data point. We then calculated the normalized response by dividing the sensor response by the output of the monochromator. We also calculated the effective transmittances of the lens by dividing the normalized response with lens by the normalized response without lens. Figures 6 and 7 show the results of our measurements. Note that this is not the actual spectral sensitivity of the photosensor as it is not corrected for non-zero offset or the variable throughput of the monochrometer. Figure 6 gives the spectral response function for the Sensor #1 (with and without lens) corrected for offset and monochrometer throughput. Figure 7 shows the approximate transmittance of the lens alone. It is reasonably flat, as would be expected for a lens exhibiting no obvious color.

Figure 8 superimposes the spectral responsivity of Sensor #1 with the photopic function (both curves normalized to unity at 555 nm). From the Figure 8, it is seen that the spectral response of Sensor #1 is similar in shape to the photopic curve but slightly narrower (80 nm fullwidth at half maximum compared to 100 nm FWHM for the photopic curve). Note also that the weighted center wavelength of the Sensor #1 is translated about 40 nm toward the blue.

To calculate the error due to the mismatch in spectral responses of the TWS sensor and a perfectly color corrected sensor (obeying the photopic curve), we use:

$$a(Z) = \frac{s_T(Z)}{s_T(N)}$$

where a(Z) is the ratio of the responsivity $s_T(Z)$ when the test sensor is irradiated with radiation Z to the responsivity $s_T(N)$ when it is irradiated with a reference radiation N. For control photosensors that work with daylight and modern fluorescent lamps, we suggest that the reference radiation N be the relative spectral response curve of a 3500 K fluorescent lamp (RE-735) and the test radiation Z be the relative spectral response of a phase of daylight (CIE Illuminant D_{65}). The error in measuring the test radiation D_{65} is:

$$f_1(D_{65}) = a(D_{65}) - 1$$
$$f_1(D_{65}) = \left(s_D / s_{35} \right) - 1$$

Expanding we get:

$$f_1(D) = \frac{\sum_{i=\min}^{\max} S(\lambda_i)_{D65} V(\lambda_i)_{rel} \Delta\lambda}{\sum_{i=\min}^{\max} S(\lambda_i)_{D65} r_T(\lambda_i)_{rel} \Delta\lambda} \bullet \frac{\sum_{i=\min}^{\max} S(\lambda_i)_{SP35} r_T(\lambda_i)_{rel} \Delta\lambda}{\sum_{i=\min}^{\max} S(\lambda_i)_{SP35} V(\lambda_i)_{rel} \Delta\lambda} - 1$$

where $S(\lambda_i)_{D65}$ is the relative spectral distribution curve for the CIE Illuminant D65, $r_T(\lambda_i)_{rel}$ is the relative spectral response of the test sensor, $V(\lambda_i)_{rel}$ is the relative photopic curve and $S(\lambda_i)_{SP35}$ is the relative spectral distribution curve for a RE-35 fluorescent lamp.

As we did not have on a hand the SPD for a RE-35 lamp, we used the SPD from a RE-41 lamp that we did have on electronic file. [We will redo the calculation once we obtain the SPD for the RE-35]. Using the SP-41 as the reference, we calculated that the TWS sensor will err on the high side by about 15% when measuring daylight.

[1] Commission Internationale De L'Eclairage, "Methods of Characterizing the Performance of Radiometers and Photometers," Publication CIE No. 53 (TC-2.2), 1982.

Table 1-Spectral Response of Sensor #1

Wavelength (nm)	With Lens	With Lens Corrected for Zero	Without Lens	Without Lens Corrected for Zero	Output of the Monochromator	With Lens Normalized	Without Lens Normalized	Effective Transmittances of Lens
610	0.016	0.000	0.018	0.000	0.584	0.000	0.000	0.000
609	0.017	0.000	0.018	0.000	0.577	0.000	0.000	0.000
608	0.017	0.000	0.018	0.000	0.571	0.000	0.000	0.000
607	0.017	0.000	0.018	0.000	0.564	0.000	0.000	0.000
606	0.017	0.000	0.018	0.000	0.558	0.000	0.000	0.000
605	0.017	0.000	0.018	0.000	0.551	0.000	0.000	0.000
604	0.017	0.000	0.018	0.000	0.545	0.000	0.000	0.000
603	0.017	0.000	0.018	0.000	0.540	0.000	0.000	0.000
602	0.017	0.000	0.018	0.000	0.534	0.000	0.000	0.000
601	0.017	0.000	0.018	0.000	0.529	0.000	0.000	0.000
600	0.017	0.000	0.018	0.000	0.523	0.000	0.000	0.000
599	0.017	0.000	0.018	0.000	0.522	0.000	0.000	0.000
598	0.017	0.000	0.018	0.000	0.522	0.000	0.000	0.000
597	0.017	0.000	0.018	0.000	0.521	0.000	0.000	0.000
596	0.017	0.000	0.018	0.000	0.521	0.000	0.000	0.000
595	0.017	0.000	0.019	0.001	0.520	0.000	0.002	0.000
594	0.017	0.000	0.019	0.001	0.509	0.000	0.002	0.000
593	0.017	0.000	0.019	0.001	0.497	0.000	0.002	0.000
592	0.017	0.000	0.020	0.002	0.486	0.000	0.004	0.000
591	0.017	0.000	0.020	0.002	0.474	0.000	0.004	0.000
590	0.017	0.000	0.021	0.003	0.463	0.000	0.006	0.000
589	0.018	0.001	0.021	0.003	0.456	0.002	0.007	3.000
588	0.018	0.001	0.022	0.004	0.450	0.002	0.009	4.000
587	0.018	0.001	0.023	0.005	0.443	0.002	0.011	5.000
586	0.018	0.001	0.024	0.006	0.437	0.002	0.014	6.000
585	0.019	0.002	0.025	0.007	0.430	0.005	0.016	3.500
584	0.019	0.002	0.026	0.008	0.423	0.005	0.019	4.000
583	0.020	0.003	0.028	0.010	0.416	0.007	0.024	3.333
582	0.020	0.003	0.030	0.012	0.409	0.007	0.029	4.000
581	0.021	0.004	0.032	0.014	0.402	0.010	0.035	3.500
580	0.021	0.004	0.034	0.016	0.395	0.010	0.041	4.000
579	0.022	0.005	0.037	0.019	0.388	0.013	0.049	3.800
578	0.023	0.006	0.040	0.022	0.382	0.016	0.058	3.667
577	0.024	0.007	0.044	0.026	0.375	0.019	0.069	3.714
576	0.026	0.009	0.049	0.031	0.369	0.024	0.084	3.444
575	0.027	0.010	0.057	0.039	0.362	0.028	0.108	3.900
574	0.029	0.012	0.063	0.045	0.354	0.034	0.127	3.750
573	0.032	0.015	0.072	0.054	0.346	0.043	0.156	3.600
572	0.034	0.017	0.082	0.064	0.338	0.050	0.189	3.765
571	0.038	0.021	0.095	0.077	0.330	0.064	0.233	3.667
570	0.042	0.025	0.108	0.090	0.322	0.078	0.280	3.600
569	0.046	0.029	0.121	0.103	0.315	0.092	0.327	3.552
568	0.049	0.032	0.135	0.117	0.307	0.104	0.381	3.656
567	0.054	0.037	0.138	0.120	0.300	0.123	0.400	3.243
566	0.057	0.040	0.160	0.142	0.292	0.137	0.486	3.550
565	0.060	0.043	0.171	0.153	0.285	0.151	0.537	3.558
564	0.064	0.047	0.181	0.163	0.278	0.169	0.587	3.468
563	0.070	0.053	0.203	0.185	0.270	0.196	0.685	3.491
562	0.075	0.058	0.227	0.209	0.263	0.221	0.795	3.603
561	0.081	0.064	0.247	0.229	0.255	0.251	0.897	3.578
560	0.087	0.070	0.265	0.247	0.248	0.282	0.996	3.529
559	0.092	0.075	0.281	0.263	0.241	0.311	1.092	3.507
558	0.096	0.079	0.294	0.276	0.234	0.338	1.182	3.494

Wavelength (nm)	With Lens	With Lens Corrected for Zero	Without Lens	Without Lens Corrected for Zero	Output of the Monochromator	With Lens Normalized	Without Lens Normalized	Effective Transmittances of Lens
557	0.100	0.083	0.303	0.285	0.226	0.367	1.259	3.434
556	0.102	0.085	0.309	0.291	0.219	0.388	1.328	3.424
555	0.103	0.086	0.307	0.289	0.212	0.406	1.363	3.360
554	0.101	0.084	0.300	0.282	0.206	0.408	1.370	3.357
553	0.096	0.079	0.278	0.260	0.200	0.396	1.303	3.291
552	0.089	0.072	0.257	0.239	0.193	0.372	1.236	3.319
551	0.083	0.066	0.234	0.216	0.187	0.353	1.154	3.273
550	0.080	0.063	0.222	0.204	0.181	0.348	1.127	3.238
549	0.076	0.059	0.209	0.191	0.176	0.336	1.086	3.237
548	0.072	0.055	0.199	0.181	0.171	0.322	1.061	3.291
547	0.069	0.052	0.187	0.169	0.165	0.314	1.022	3.250
546	0.066	0.049	0.177	0.159	0.160	0.306	0.993	3.245
545	0.064	0.047	0.168	0.150	0.155	0.303	0.968	3.191
544	0.062	0.045	0.161	0.143	0.151	0.298	0.948	3.178
543	0.060	0.043	0.154	0.136	0.147	0.293	0.928	3.163
542	0.059	0.042	0.150	0.132	0.142	0.295	0.927	3.143
541	0.058	0.041	0.144	0.126	0.138	0.297	0.912	3.073
540	0.057	0.040	0.140	0.122	0.134	0.299	0.910	3.050
539	0.056	0.039	0.136	0.118	0.131	0.298	0.902	3.026
538	0.055	0.038	0.132	0.114	0.128	0.298	0.893	3.000
537	0.054	0.037	0.129	0.111	0.124	0.297	0.892	3.000
536	0.053	0.036	0.125	0.107	0.121	0.297	0.883	2.972
535	0.053	0.036	0.122	0.104	0.118	0.305	0.881	2.889
534	0.052	0.035	0.119	0.101	0.115	0.303	0.875	2.886
533	0.051	0.034	0.116	0.098	0.113	0.301	0.869	2.882
532	0.051	0.034	0.114	0.096	0.110	0.309	0.871	2.824
531	0.050	0.033	0.112	0.094	0.108	0.307	0.874	2.848
530	0.049	0.032	0.109	0.091	0.105	0.305	0.867	2.844
529	0.049	0.032	0.108	0.090	0.103	0.310	0.872	2.813
528	0.048	0.031	0.106	0.088	0.101	0.306	0.868	2.839
527	0.048	0.031	0.104	0.086	0.100	0.311	0.863	2.774
526	0.047	0.030	0.102	0.084	0.098	0.307	0.859	2.800
525	0.047	0.030	0.101	0.083	0.096	0.313	0.865	2.767
524	0.046	0.029	0.100	0.082	0.095	0.307	0.867	2.828
523	0.046	0.029	0.098	0.080	0.093	0.311	0.858	2.759
522	0.045	0.028	0.097	0.079	0.092	0.305	0.861	2.821
521	0.045	0.028	0.095	0.077	0.090	0.310	0.852	2.750
520	0.044	0.027	0.094	0.076	0.089	0.303	0.854	2.815
519	0.044	0.027	0.094	0.076	0.087	0.310	0.872	2.815
518	0.044	0.027	0.093	0.075	0.085	0.316	0.878	2.778
517	0.043	0.026	0.091	0.073	0.084	0.311	0.873	2.808
516	0.042	0.025	0.088	0.070	0.082	0.306	0.856	2.800
515	0.042	0.025	0.085	0.067	0.080	0.313	0.838	2.680
514	0.041	0.024	0.083	0.065	0.078	0.307	0.831	2.708
513	0.040	0.023	0.082	0.064	0.076	0.301	0.838	2.783
512	0.040	0.023	0.080	0.062	0.075	0.308	0.831	2.696
511	0.039	0.022	0.078	0.060	0.073	0.302	0.824	2.727
510	0.039	0.022	0.076	0.058	0.071	0.310	0.817	2.636
509	0.038	0.021	0.074	0.056	0.070	0.302	0.805	2.667
508	0.038	0.021	0.073	0.055	0.068	0.308	0.806	2.619
507	0.037	0.020	0.071	0.053	0.067	0.299	0.793	2.650
506	0.036	0.019	0.070	0.052	0.065	0.291	0.795	2.737
505	0.036	0.019	0.067	0.049	0.064	0.297	0.766	2.579
504	0.035	0.018	0.066	0.048	0.063	0.288	0.767	2.667
503	0.035	0.018	0.065	0.047	0.061	0.294	0.768	2.611
502	0.034	0.017	0.063	0.045	0.060	0.284	0.753	2.647

Wavelength (nm)	With Lens	With Lens Corrected for Zero	Without Lens	Without Lens Corrected for Zero	Output of the Monochromator	With Lens Normalized	Without Lens Normalized	Effective Transmittances of Lens
501	0.034	0.017	0.062	0.044	0.058	0.291	0.753	2.588
500	0.033	0.016	0.061	0.043	0.057	0.281	0.754	2.688
499	0.032	0.015	0.060	0.042	0.056	0.268	0.750	2.800
498	0.033	0.016	0.059	0.041	0.055	0.291	0.745	2.563
497	0.032	0.015	0.058	0.040	0.054	0.278	0.741	2.667
496	0.032	0.015	0.056	0.038	0.053	0.283	0.717	2.533
495	0.031	0.014	0.055	0.037	0.052	0.269	0.712	2.643
494	0.031	0.014	0.054	0.036	0.051	0.275	0.706	2.571
493	0.030	0.013	0.053	0.035	0.050	0.260	0.700	2.692
492	0.030	0.013	0.052	0.034	0.049	0.265	0.694	2.615
491	0.029	0.012	0.051	0.033	0.048	0.250	0.688	2.750
490	0.029	0.012	0.049	0.031	0.047	0.255	0.660	2.583
489	0.029	0.012	0.048	0.030	0.046	0.260	0.649	2.500
488	0.028	0.011	0.047	0.029	0.045	0.242	0.639	2.636
487	0.028	0.011	0.046	0.028	0.045	0.247	0.628	2.545
486	0.027	0.010	0.045	0.027	0.044	0.228	0.616	2.700
485	0.027	0.010	0.044	0.026	0.043	0.233	0.605	2.600
484	0.026	0.009	0.043	0.025	0.042	0.213	0.592	2.778
483	0.026	0.009	0.042	0.024	0.041	0.217	0.580	2.667
482	0.026	0.009	0.040	0.022	0.041	0.222	0.542	2.444
481	0.025	0.008	0.039	0.021	0.040	0.201	0.528	2.625
480	0.025	0.008	0.038	0.020	0.039	0.205	0.513	2.500
470	0.021	0.004	0.029	0.011	0.033	0.121	0.333	2.750
460	0.019	0.002	0.023	0.005	0.028	0.071	0.179	2.500
450	0.017	0.000	0.019	0.001	0.023	0.000	0.043	0.000
440	0.017	0.000	0.018	0.000	0.019	0.000	0.000	0.000

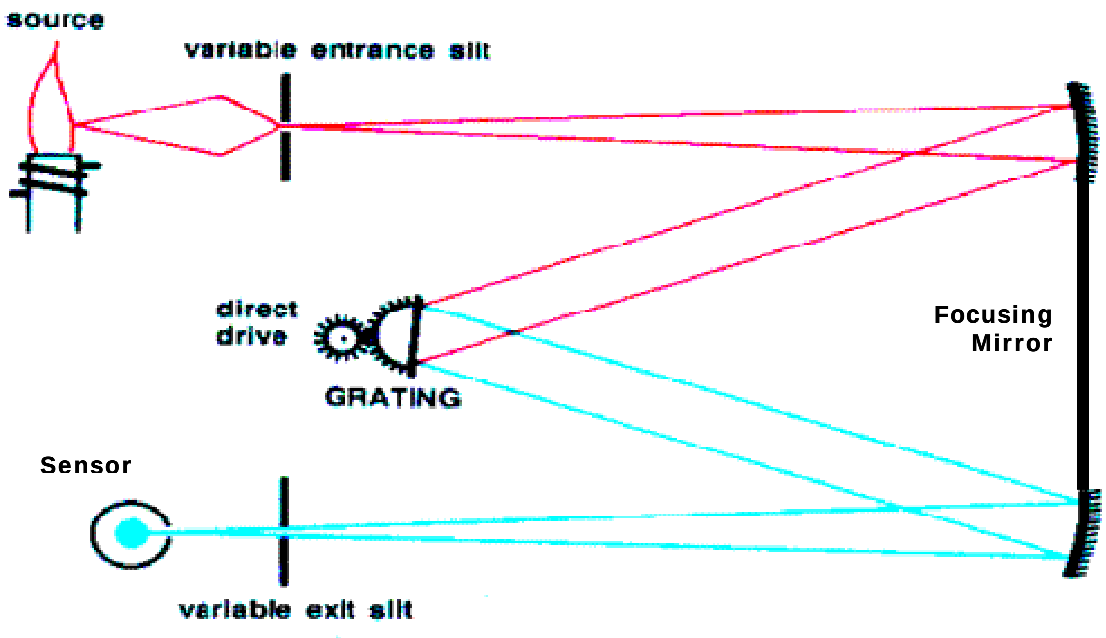

Figure 1-Principle of the Ebert monochromator

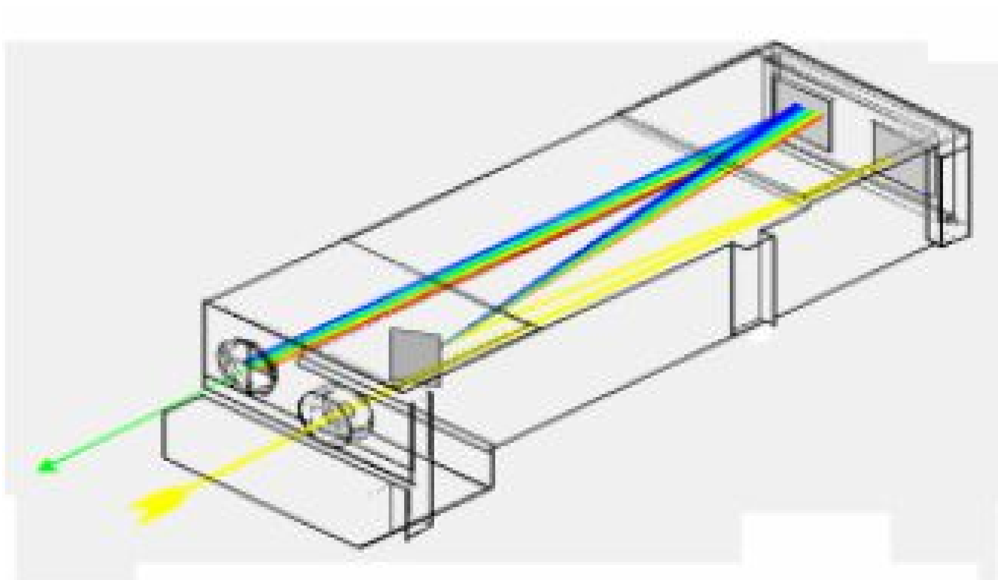

Figure 2-Ebert monochromator, consists of fixed entrance and exit slits, fixed focusing mirror and a rotatable diffraction grating. As the grating rotates a different wavelength is focused onto the exit slit.

Figure 3-Ebert monochromator – model JA 82-000

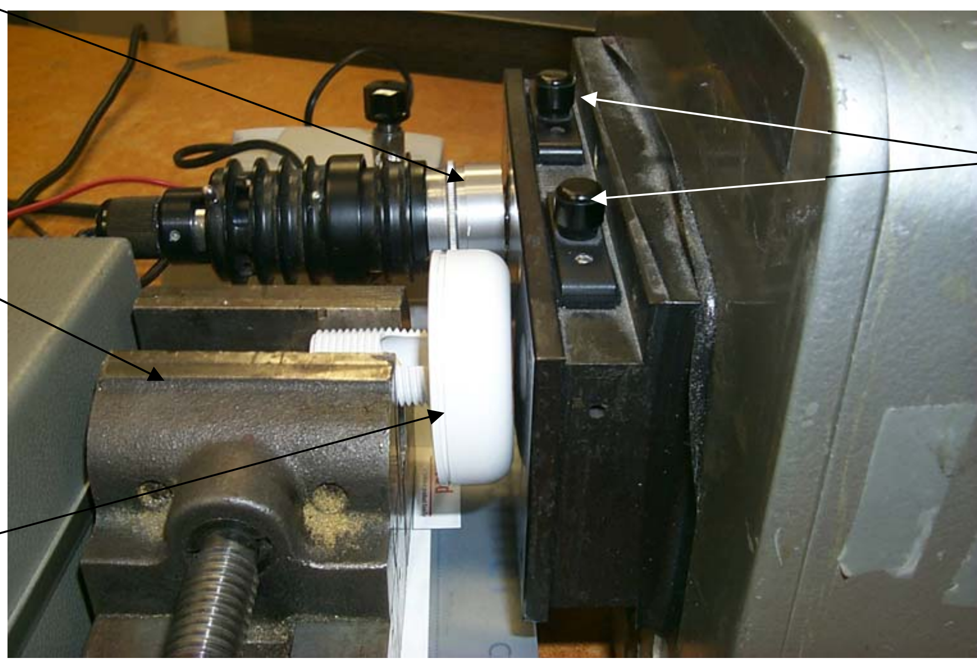

Figure 4-Monochromator Sample and Light source position

Figure 5-Monochromator Output

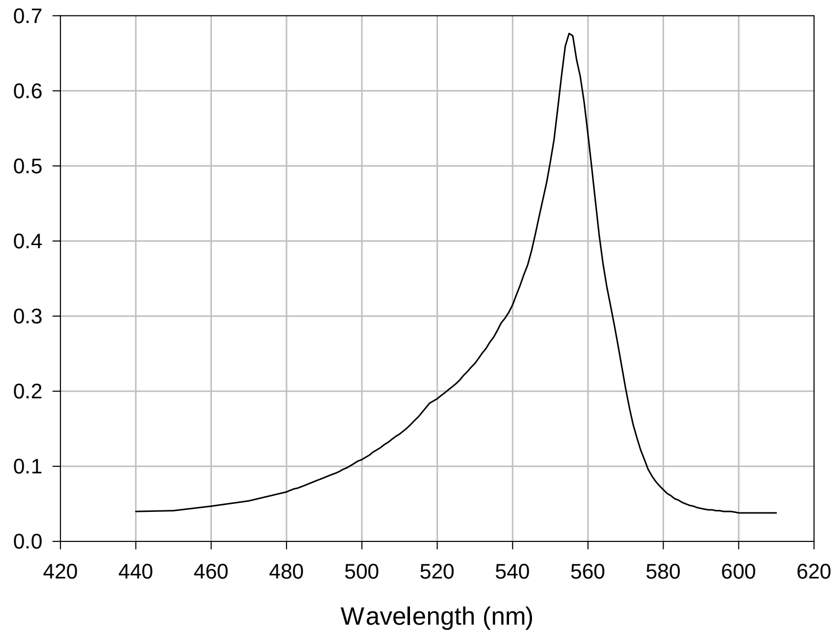

Figure 6-Spectral Response
Wattstoper Sensor#1 Corrected for Zero & Normalized

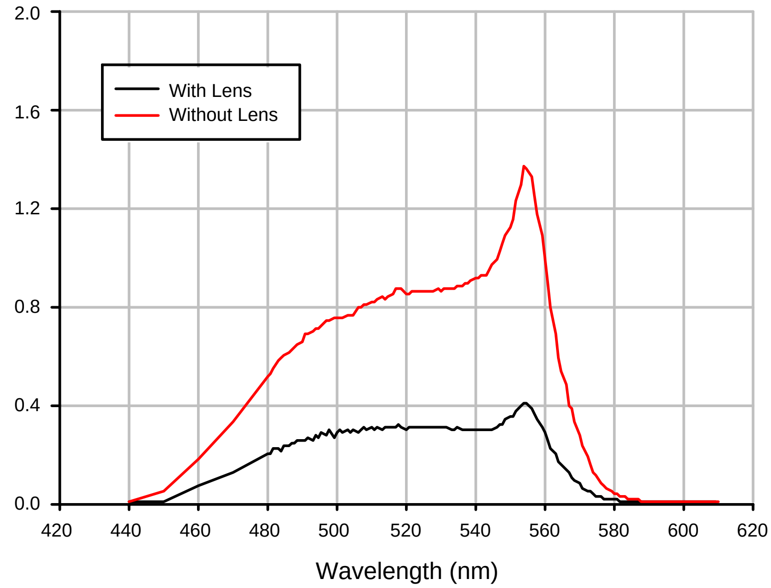

Figure 7-Sensor#1Effective Transmittances of Lens

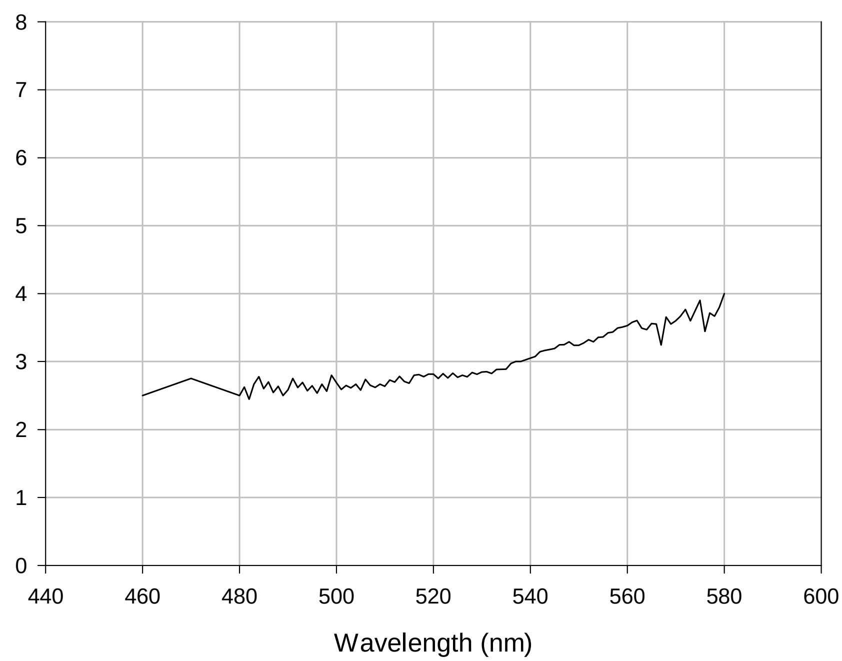

Figure 8
Spectral Response of Photocell Compared to Photopic Curve

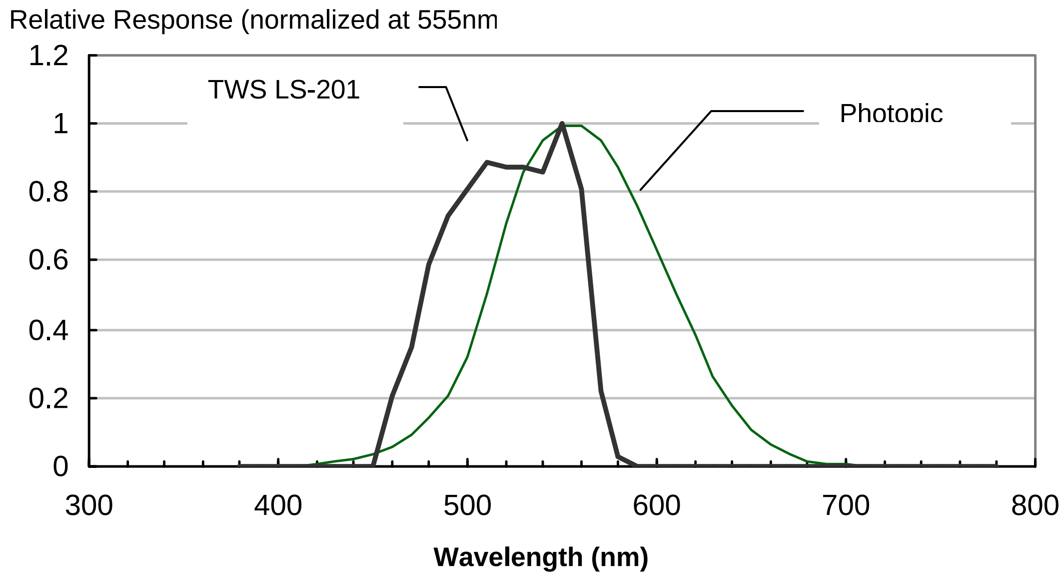

Characterizing the Spatial Performance

One factor affecting the performance of a control photosensor is its sensitivity to light striking it from different directions. The spatial response function (SRF) describes the sensitivity of the photosensor to incident radiation from coming from different directions within a space. Previous work has shown that SRFs differ from photosensor to photosensor. In some cases, the photocell viewed nearly an entire hemisphere with a roughly cosine response while others selectively sampled the space in different directions. It has also been shown the SRF and photosensor placement significantly affect overall control system performance particularly in cases where incorrect control algorithms are employed (viz. using integral reset for daylighting applications). In extreme cases, poorly designed systems can let light levels fall too far, causing occupant complaints and even sabotage.

In project 3.3, the LBNL Lighting Lab is assisting The Watt Stopper by measuring the spatial response function of candidate photosensors. The purpose of these measurements was to characterize the spatial performance of the photosensor by measuring the angular response of the photosensor to incident light.

Method

The spatial response of the photosensor was measured by affixing it at the photometric center of a miniature goniometer and subjecting the sensor to a light mounted to the movable arm. We used a two-axis goniometer (Figures 9 and 10) that was originally developed to measure the spatial distribution of light from novel light emitting diodes (LEDs). The goniophotometer, which consists of two perpendicular rotary stages which rotate around the vertical axis, measuring altitude, ψ, and the horizontal axis, measuring azimuth, θ. The two angles, ψ and θ, defined the direction of light incident on the photosensor. We used the computer program Labview to program two stepper motors, through the serial port of the computer, to step the altitude angle, from –100 to 100 degrees, for all rotations of the azimuth angle. Measurements were taken every 10 degrees for both the altitude and azimuth axes. For each pair of altitude and azimuth angles (ψ ,θ), we measured the response of the sensor. This method is exactly equivalent to the accepted method used to characterize the candlepower distribution from luminaries. The photosensor was mounted on the goniometer such that the center of the sensor was at the center of rotation. We used an aligning telescope to center the sensor. The distance between the sensor and the light source was 7cm (Figure 10). The light source we used was a 3-Watt, clear incandescent 1487 pilot light. We used a regulated voltage source so that the light did not vary during the test. The output of the sensor (measured in volts) was read back into the computer, through a National Instrument data acquisition board (DAQ PCI-6034E), and was displayed on the Labview screen.

We measured the spatial response of two LS201, with and without lens. These photosensors had been modified by The Watt Stopper before the test so that the photosensors acted like meters (rather than as active control photosensors, which would have rendered accurate readings of the response impossible). For all the measurements, we covered the sensor and the light source with a wooden box painted black internally to minimize any light reflections within the system.

Results of the Spatial Response Testing

For this report, we included the results for both sensors. The tabulated data results are summarized in Tables 2 through 5 and key spatial characteristics given in Figures 12,13, 14, and 15. Tables 2 through 5 list the results of the sensor response, both with the lens and with the lens removed. For each altitude angle, we averaged the angular response of the sensor over azimuth planes. We then calculated the normalized response by dividing the average of the sensor response by the average response at zero degree altitude angle. We also calculated the cosine response to demonstrate that the sensors have a much narrower cone of acceptance than a cosine response. Figures 12 though 15 show the normalized and cosine response for each sensor with and without lens.

Table 2-Spatial response of Sensor #1 With Lens

Azimuth →	-90	-80	-70	-60	-50	-40	-30	-20	-10	0	10
Altitude											
0	8.30	8.30	8.30	8.30	8.30	8.30	8.30	8.30	8.30	8.30	8.30
10	3.43	3.32	3.23	3.18	3.15	3.15	3.18	3.25	3.36	3.43	3.32
20	1.36	1.32	1.28	1.25	1.21	1.19	1.17	1.17	1.18	1.36	1.32
30	0.80	0.78	0.76	0.73	0.71	0.70	0.69	0.68	0.68	0.80	0.78
40	0.47	0.46	0.45	0.44	0.43	0.43	0.43	0.43	0.43	0.47	0.46
50	0.19	0.19	0.19	0.19	0.19	0.20	0.20	0.20	0.20	0.19	0.19
60	0.10	0.10	0.10	0.10	0.10	0.10	0.11	0.11	0.11	0.10	0.10
70	0.05	0.05	0.05	0.05	0.05	0.05	0.05	0.06	0.06	0.05	0.05
80	0.03	0.03	0.03	0.03	0.03	0.03	0.03	0.03	0.03	0.03	0.03
90	0.03	0.03	0.03	0.03	0.03	0.03	0.03	0.03	0.03	0.03	0.03

Table 2- Continued

Azimuth →	20	30	40	50	60	70	80	90	100	110	120
Altitude											
0	8.30	8.30	8.30	8.30	8.30	8.30	8.30	8.30	8.30	8.30	8.30
10	3.99	4.27	4.63	5.06	5.61	6.27	7.03	8.30	8.30	8.30	8.30
20	1.27	1.33	1.40	1.50	1.62	1.75	1.89	3.51	3.69	3.91	3.94
30	0.70	0.72	0.75	0.79	0.83	0.89	0.93	1.29	1.33	1.37	1.40
40	0.44	0.45	0.47	0.49	0.51	0.53	0.55	0.73	0.75	0.78	0.80
50	0.21	0.22	0.22	0.23	0.24	0.24	0.25	0.41	0.42	0.44	0.45
60	0.11	0.11	0.11	0.11	0.11	0.11	0.11	0.15	0.15	0.15	0.15
70	0.06	0.06	0.06	0.06	0.06	0.06	0.06	0.08	0.08	0.07	0.07
80	0.03	0.03	0.03	0.03	0.03	0.03	0.03	0.04	0.04	0.04	0.04
90	0.03	0.03	0.03	0.03	0.03	0.03	0.03	0.03	0.03	0.03	0.03

Table 2- Continued

Azimuth →	130	140	150	160	170	180	190	200	210	220	230
Altitude											
0	8.30	8.30	8.30	8.30	8.30	8.30	8.30	8.30	8.30	8.30	8.30
10	8.30	8.30	8.30	8.30	8.30	8.29	8.30	8.30	8.30	8.30	7.75
20	3.99	3.88	3.79	3.57	3.40	3.15	2.94	2.70	2.54	2.37	2.24
30	1.43	1.43	1.43	1.40	1.39	1.34	1.30	1.25	1.22	1.17	1.14
40	0.82	0.83	0.83	0.83	0.83	0.82	0.80	0.77	0.75	0.73	0.71
50	0.46	0.46	0.46	0.45	0.45	0.44	0.44	0.42	0.41	0.39	0.38
60	0.14	0.14	0.14	0.14	0.13	0.13	0.13	0.13	0.13	0.12	0.12
70	0.07	0.07	0.07	0.07	0.07	0.07	0.07	0.07	0.07	0.06	0.07
80	0.04	0.04	0.04	0.04	0.04	0.04	0.04	0.04	0.04	0.04	0.04
90	0.03	0.03	0.03	0.03	0.03	0.03	0.03	0.03	0.03	0.03	0.03

Table 2- Continued

Azimuth →	240	250	260	Average Response	Normalized Response	Cosine Response
Altitude						
0	8.30	8.30	8.30	8.300	1.000	1.000
10	7.19	6.73	6.38	6.045	0.728	0.985
20	2.10	2.00	1.90	2.220	0.267	0.940
30	1.09	1.05	1.00	1.015	0.122	0.866
40	0.68	0.65	0.62	0.611	0.074	0.766
50	0.35	0.34	0.32	0.313	0.038	0.643
60	0.12	0.12	0.12	0.120	0.014	0.500
70	0.07	0.07	0.07	0.063	0.008	0.342
80	0.04	0.04	0.03	0.035	0.004	0.174
90	0.03	0.03	0.03	0.030	0.004	0.000

Table 3-Spatial response of Sensor #1 Without Lens

Azimuth →	-90	-80	-70	-60	-50	-40	-30	-20	-10	0	10
Altitude											
0	4.64	4.62	4.61	5.47	5.49	5.49	5.50	5.47	5.44	5.51	5.53
10	4.13	4.01	3.95	4.68	4.72	4.75	4.69	4.52	4.32	4.24	4.10
20	3.32	3.42	3.56	4.44	4.31	4.22	4.00	3.72	3.47	3.41	3.45
30	2.02	1.95	1.70	1.69	1.51	1.42	1.21	1.10	1.11	1.16	1.12
40	0.75	0.75	0.72	0.82	0.74	0.70	0.68	0.70	0.76	0.81	0.79
50	0.59	0.58	0.59	0.70	0.65	0.61	0.60	0.59	0.66	0.70	0.69
60	0.52	0.51	0.52	0.60	0.59	0.52	0.49	0.50	0.57	0.61	0.60
70	0.45	0.44	0.25	0.35	0.30	0.25	0.22	0.25	0.29	0.61	0.61
80	0.16	0.22	0.24	0.21	0.21	0.15	0.13	0.15	0.15	0.17	0.19
90	0.08	0.06	0.07	0.08	0.20	0.07	0.12	0.18	0.22	0.19	0.32

Table 3- Continued

Azimuth →	20	30	40	50	60	70	80	90	100	110	120
Altitude											
0	5.54	5.57	5.61	5.66	5.72	5.79	5.87	4.64	4.62	4.61	5.47
10	4.01	4.12	4.34	4.51	4.56	4.74	4.88	4.43	4.49	5.48	5.86
20	3.34	3.39	3.51	3.86	4.17	4.59	4.97	5.23	5.05	5.90	6.06
30	1.12	1.14	1.15	1.15	1.16	1.22	1.31	2.34	2.62	3.62	3.98
40	0.78	0.77	0.78	0.78	0.80	0.83	0.90	0.86	0.94	1.18	1.22
50	0.67	0.65	0.64	0.64	0.64	0.66	0.69	0.63	0.64	0.75	0.81
60	0.59	0.60	0.57	0.56	0.54	0.56	0.57	0.49	0.48	0.61	0.69
70	0.62	0.60	0.58	0.55	0.49	0.50	0.54	0.43	0.43	0.55	0.14
80	0.46	0.53	0.46	0.24	0.30	0.47	0.44	0.37	0.36	0.37	0.29
90	0.31	0.41	0.16	0.23	0.31	0.10	0.11	0.27	0.11	0.33	0.33

Table 3- Continued

Azimuth →	130	140	150	160	170	180	190	200	210	220	230
Altitude											
0	5.49	5.49	5.50	5.47	5.44	5.51	5.53	5.54	5.57	5.61	5.66
10	6.22	6.38	6.35	6.16	6.03	5.95	5.81	5.74	5.74	5.77	5.66
20	6.40	6.75	7.03	7.00	6.88	6.58	5.94	5.55	5.19	4.99	4.80
30	4.56	5.08	5.54	5.65	5.83	6.01	5.76	5.47	5.60	5.77	5.76
40	1.36	1.48	1.61	1.68	1.60	1.55	1.38	1.10	1.01	1.36	1.55
50	0.86	1.06	1.06	0.94	0.77	0.62	0.68	0.75	0.77	0.77	0.73
60	0.71	0.84	0.92	0.75	0.61	0.53	0.65	0.67	0.62	0.59	0.58
70	0.13	0.40	0.14	0.27	0.50	0.53	0.56	0.54	0.52	0.51	0.49
80	0.19	0.14	0.10	0.15	0.48	0.60	0.55	0.52	0.54	0.49	0.30
90	0.22	0.07	0.06	0.11	0.46	0.16	0.08	0.07	0.35	0.12	0.08

Table 3- Continued

Azimuth → / Altitude	240	250	260	Average Response	Normalized Response	Cosine Response
0	5.72	5.79	5.87	5.418	1.000	1.000
10	5.39	5.15	5.03	5.025	0.927	0.985
20	4.48	4.11	3.93	4.751	0.877	0.940
30	5.12	4.40	3.80	3.088	0.570	0.866
40	1.38	1.25	1.17	1.043	0.192	0.766
50	0.70	0.69	0.72	0.708	0.131	0.643
60	0.57	0.59	0.60	0.598	0.110	0.500
70	0.49	0.52	0.53	0.433	0.080	0.342
80	0.18	0.17	0.19	0.302	0.056	0.174
90	0.07	0.11	0.11	0.176	0.032	0.000

Table 4-Spatial response of Sensor #2 With Lens

Azimuth →	-90	-80	-70	-60	-50	-40	-30	-20	-10	0	10
Altitude											
0	4.75	4.70	4.68	4.68	4.69	4.72	4.77	4.84	4.93	5.03	5.15
10	1.51	1.52	1.53	1.54	1.57	1.62	1.67	1.73	1.80	1.86	1.94
20	0.57	0.57	0.58	0.58	0.59	0.60	0.60	0.61	0.61	0.62	0.63
30	0.34	0.33	0.34	0.34	0.34	0.35	0.35	0.35	0.35	0.35	0.35
40	0.23	0.24	0.24	0.24	0.24	0.24	0.24	0.25	0.25	0.25	0.25
50	0.16	0.16	0.16	0.16	0.16	0.16	0.17	0.17	0.17	0.17	0.17
60	0.09	0.09	0.09	0.09	0.09	0.10	0.10	0.10	0.10	0.10	0.10
70	0.07	0.07	0.07	0.07	0.08	0.08	0.08	0.08	0.08	0.08	0.07
80	0.06	0.06	0.06	0.06	0.06	0.06	0.06	0.06	0.06	0.06	0.06
90	0.06	0.06	0.06	0.06	0.06	0.06	0.06	0.06	0.06	0.06	0.06

Table 4- Continued

Azimuth →	20	30	40	50	60	70	80	90	100	110	120
Altitude											
0	5.28	5.41	5.55	5.69	5.82	5.94	6.04	4.75	4.70	4.68	4.68
10	2.03	2.14	2.28	2.45	2.63	2.81	2.96	4.92	4.96	4.94	4.85
20	0.65	0.67	0.70	0.73	0.77	0.81	0.84	1.42	1.41	1.41	1.37
30	0.35	0.35	0.36	0.37	0.39	0.39	0.40	0.51	0.50	0.51	0.50
40	0.25	0.25	0.26	0.26	0.27	0.27	0.27	0.30	0.30	0.30	0.30
50	0.18	0.18	0.18	0.18	0.18	0.18	0.18	0.20	0.20	0.20	0.20
60	0.10	0.10	0.10	0.09	0.09	0.09	0.09	0.10	0.09	0.09	0.09
70	0.07	0.07	0.07	0.07	0.07	0.07	0.07	0.07	0.07	0.07	0.07
80	0.06	0.06	0.06	0.06	0.06	0.06	0.06	0.06	0.06	0.06	0.06
90	0.06	0.06	0.06	0.06	0.06	0.06	0.06	0.06	0.06	0.06	0.06

Table 4- Continued

Azimuth →	130	140	150	160	170	180	190	200	210	220	230
Altitude											
0	4.69	4.72	4.77	4.84	4.93	5.03	5.15	5.28	5.41	5.55	5.69
10	4.70	4.49	4.24	3.97	3.70	3.45	3.22	3.03	2.88	2.76	2.67
20	1.34	1.28	1.23	1.16	1.10	1.03	0.97	0.92	0.89	0.85	0.84
30	0.50	0.50	0.50	0.48	0.47	0.45	0.44	0.43	0.42	0.41	0.40
40	0.30	0.31	0.31	0.31	0.30	0.29	0.29	0.28	0.28	0.27	0.27
50	0.19	0.19	0.19	0.19	0.19	0.19	0.19	0.18	0.18	0.18	0.18
60	0.09	0.09	0.09	0.09	0.09	0.09	0.09	0.09	0.09	0.09	0.09
70	0.07	0.07	0.07	0.07	0.07	0.07	0.07	0.07	0.07	0.07	0.07
80	0.06	0.06	0.06	0.06	0.06	0.06	0.06	0.06	0.06	0.06	0.06
90	0.06	0.06	0.06	0.06	0.06	0.06	0.06	0.06	0.06	0.06	0.06

Table 4- Continued

Azimuth →	240	250	260	Average Response	Normalized Response	Cosine Response
Altitude						
0	5.82	5.94	6.04	5.148	1.000	1.000
10	2.61	2.57	2.55	2.836	0.551	0.985
20	0.82	0.82	0.81	0.872	0.169	0.940
30	0.40	0.39	0.39	0.406	0.079	0.866
40	0.26	0.26	0.26	0.269	0.052	0.766
50	0.18	0.18	0.18	0.179	0.035	0.643
60	0.09	0.09	0.10	0.093	0.018	0.500
70	0.07	0.07	0.07	0.072	0.014	0.342
80	0.06	0.06	0.06	0.060	0.012	0.174
90	0.06	0.06	0.06	0.060	0.012	0.000

Table 5-Spatial response of Sensor #2 Without Lens

Azimuth →	-90	-80	-70	-60	-50	-40	-30	-20	-10	0	10
Altitude											
0	1.82	1.83	1.86	1.89	1.91	1.93	1.93	1.94	1.93	1.93	1.92
10	1.93	1.90	1.87	1.86	1.86	1.89	1.91	1.94	1.93	1.91	1.96
20	1.41	1.37	1.29	1.27	1.31	1.33	1.29	1.29	1.33	1.37	1.42
30	0.59	0.65	0.63	0.59	0.57	0.55	0.51	0.52	0.50	0.50	0.44
40	0.30	0.32	0.32	0.32	0.33	0.33	0.32	0.33	0.33	0.34	0.34
50	0.31	0.31	0.31	0.31	0.30	0.30	0.30	0.29	0.29	0.29	0.29
60	0.29	0.30	0.30	0.34	0.28	0.28	0.27	0.27	0.26	0.27	0.27
70	0.28	0.27	0.28	0.30	0.27	0.27	0.26	0.26	0.25	0.26	0.26
80	0.28	0.28	0.27	0.27	0.26	0.27	0.26	0.26	0.27	0.28	0.27
90	0.25	0.25	0.23	0.23	0.15	0.12	0.14	0.12	0.11	0.25	0.23

Table 5- Continued

Azimuth →	20	30	40	50	60	70	80	90	100	110	120
Altitude											
0	1.92	1.91	1.92	1.93	1.94	1.96	1.98	1.82	1.83	1.86	1.89
10	1.96	1.93	1.96	2.06	2.08	2.13	2.19	1.87	1.90	1.93	1.93
20	1.57	1.66	1.87	1.96	1.97	2.08	2.14	2.36	2.38	2.41	2.51
30	0.42	0.40	0.45	0.52	0.58	0.61	0.65	1.08	1.01	1.05	1.10
40	0.31	0.29	0.31	0.33	0.33	0.35	0.36	0.39	0.39	0.38	0.37
50	0.27	0.26	0.26	0.27	0.28	0.28	0.29	0.26	0.26	0.23	0.23
60	0.25	0.24	0.24	0.25	0.26	0.27	0.27	0.24	0.23	0.21	0.20
70	0.24	0.22	0.23	0.25	0.26	0.27	0.28	0.22	0.22	0.21	0.19
80	0.24	0.22	0.22	0.24	0.24	0.24	0.22	0.22	0.20	0.15	0.12
90	0.11	0.11	0.10	0.21	0.12	0.10	0.11	0.10	0.09	0.09	0.10

Table 5- Continued

Azimuth →	130	140	150	160	170	180	190	200	210	220	230
Altitude											
0	1.91	1.93	1.93	1.94	1.93	1.93	1.92	1.92	1.91	1.92	1.93
10	1.94	1.97	1.96	1.95	1.91	1.88	1.83	1.79	1.79	1.81	1.81
20	2.56	2.56	2.49	2.41	2.26	2.09	1.98	1.88	1.78	1.70	1.62
30	1.21	1.36	1.60	1.58	1.43	1.30	1.30	1.29	1.31	1.19	0.99
40	0.39	0.42	0.46	0.47	0.45	0.42	0.40	0.39	0.37	0.36	0.33
50	0.25	0.27	0.30	0.31	0.29	0.27	0.27	0.27	0.26	0.26	0.27
60	0.21	0.22	0.21	0.21	0.25	0.25	0.24	0.24	0.23	0.23	0.25
70	0.21	0.22	0.24	0.21	0.25	0.24	0.22	0.22	0.21	0.22	0.23
80	0.16	0.19	0.21	0.21	0.25	0.24	0.22	0.22	0.23	0.24	0.26
90	0.10	0.12	0.11	0.12	0.24	0.18	0.10	0.10	0.16	0.25	0.24

Table 5- Continued

Azimuth →	240	250	260	Average Response	Normalized Response	Cosine Response
Altitude						
0	1.94	1.96	1.98	1.914	1.000	1.000
10	1.79	1.77	1.80	1.914	1.000	0.985
20	1.58	1.56	1.59	1.824	0.953	0.940
30	0.81	0.86	0.92	0.863	0.451	0.866
40	0.30	0.28	0.29	0.353	0.185	0.766
50	0.27	0.27	0.29	0.279	0.146	0.643
60	0.26	0.27	0.27	0.254	0.133	0.500
70	0.25	0.25	0.25	0.244	0.127	0.342
80	0.26	0.25	0.25	0.235	0.123	0.174
90	0.11	0.14	0.26	0.154	0.081	0.000

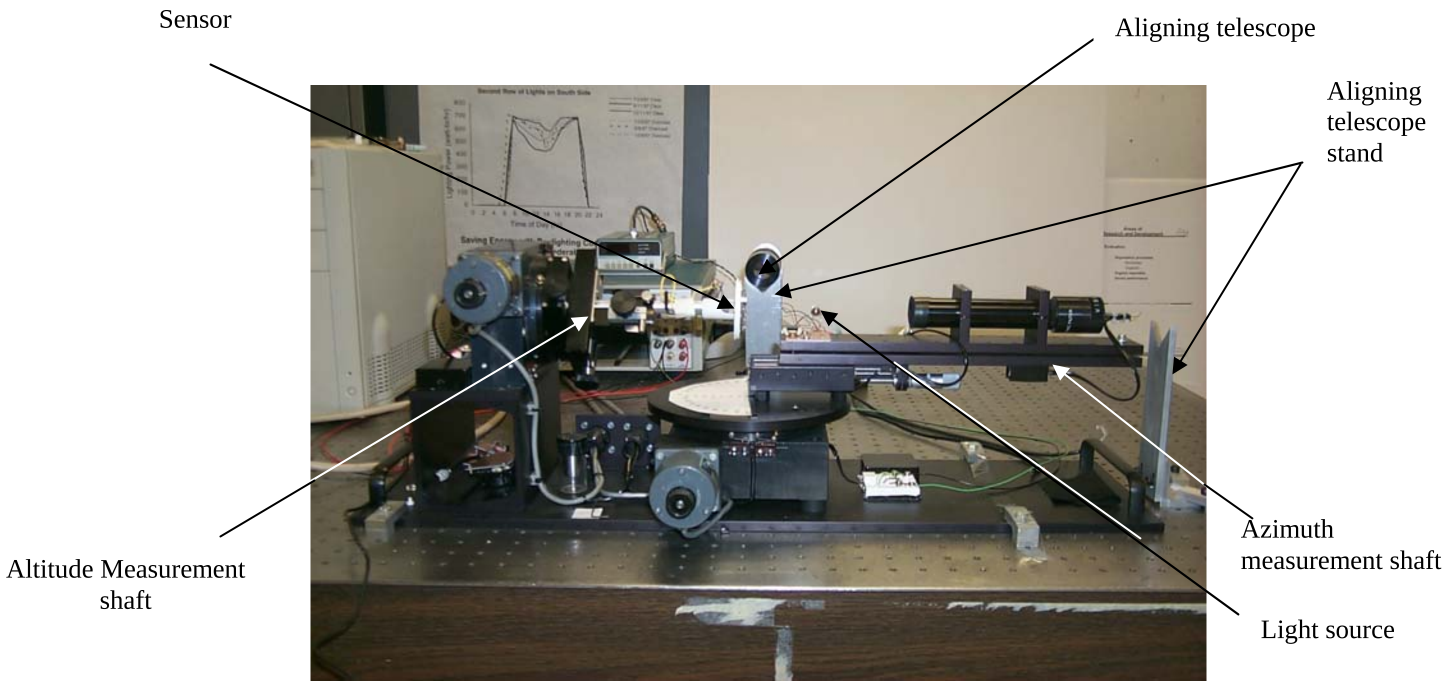

Figure 9- Goniometer used in spatial response measurement

Figure 10- Position of sensor in spatial measurement (shown with sensor's front cover removed)

Figure 11- Sensor and light source position in spatial measurements (shown with the front cover of the sensor removed.)

Figure 12-Spatial Response for Sensor #1 with Lens
Response Averaged Over All Azimuth Planes

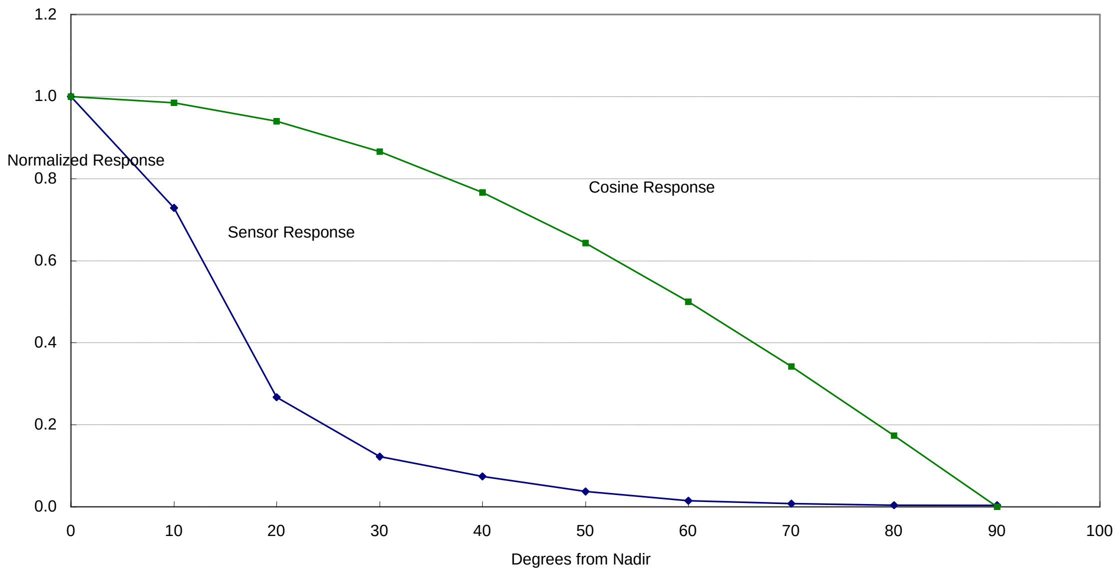

Figure 13-Spatial Response for Sensor #1 without Lens
Response Averaged Over All Azimuth Planes

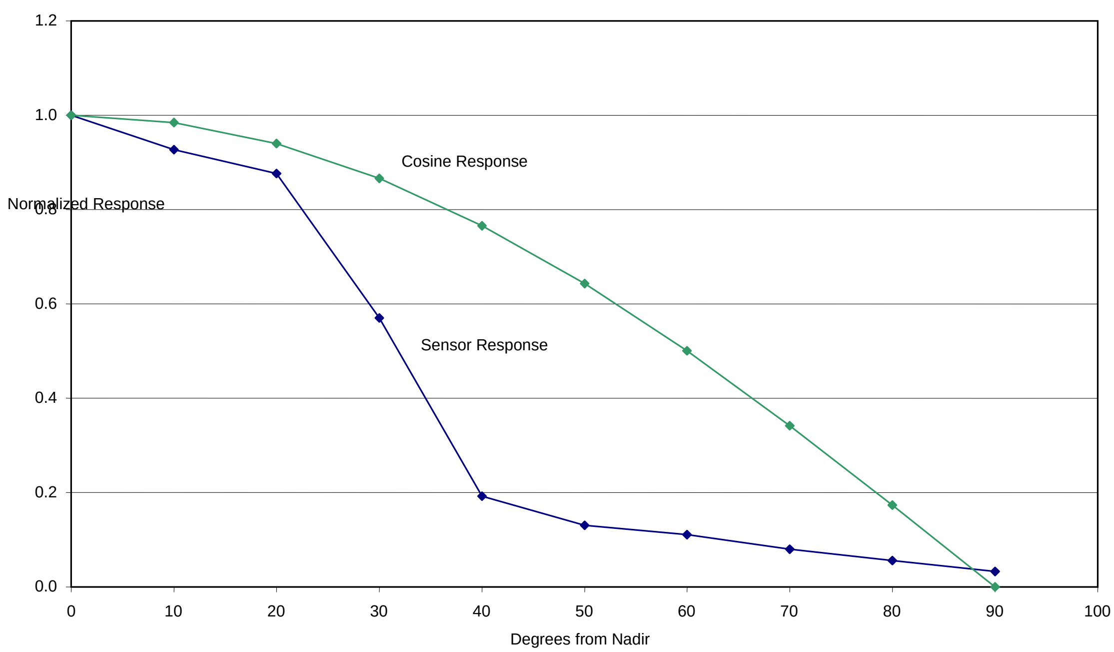

Figure 14-Spatial Response for Sensor #2 with Lens

Response Averaged Over All Azimuth Planes

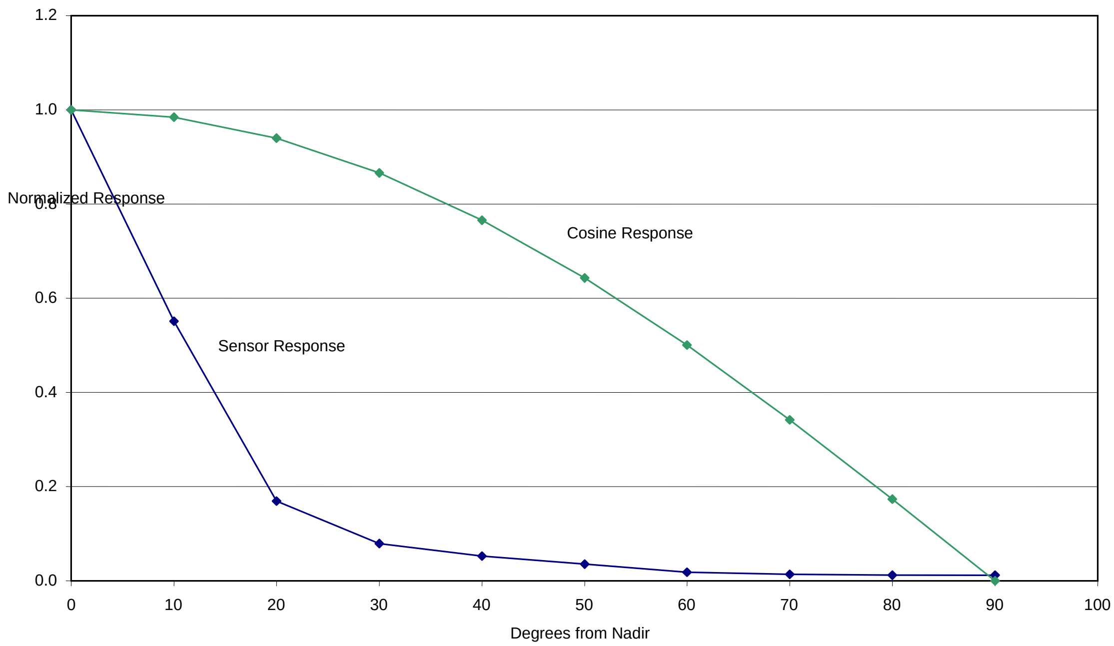

Figure 15-Spatial Response for Sensor #2 without Lens

Response Averaged Over All Azimuth Planes

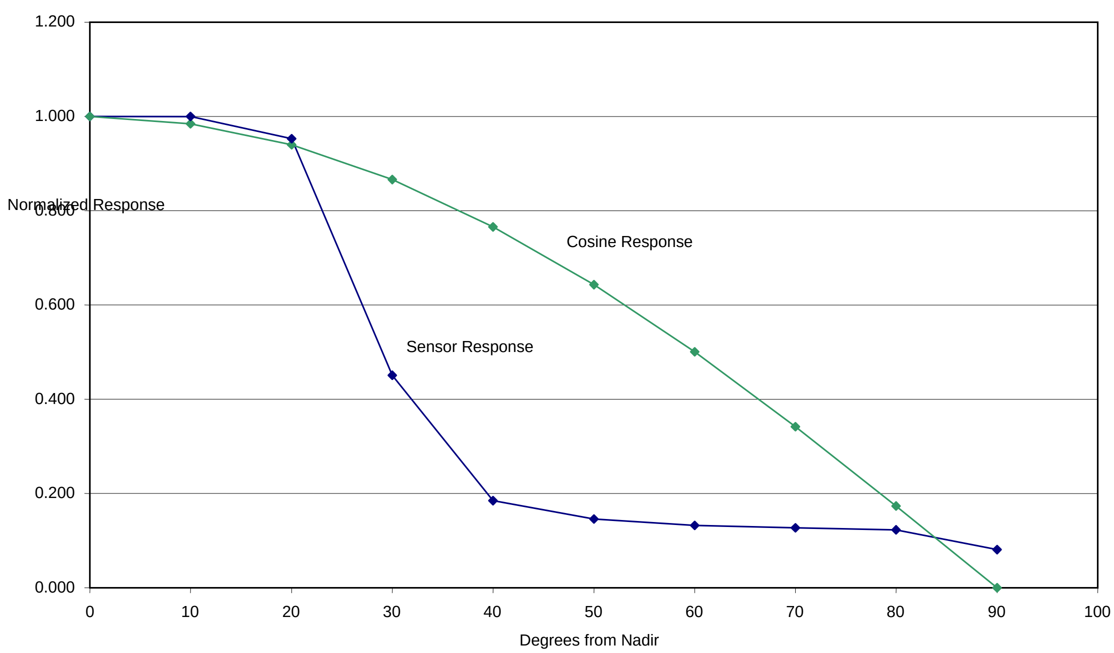

Figure 16. Polar Plot of Spatial Responsivity Function of Sensor #1

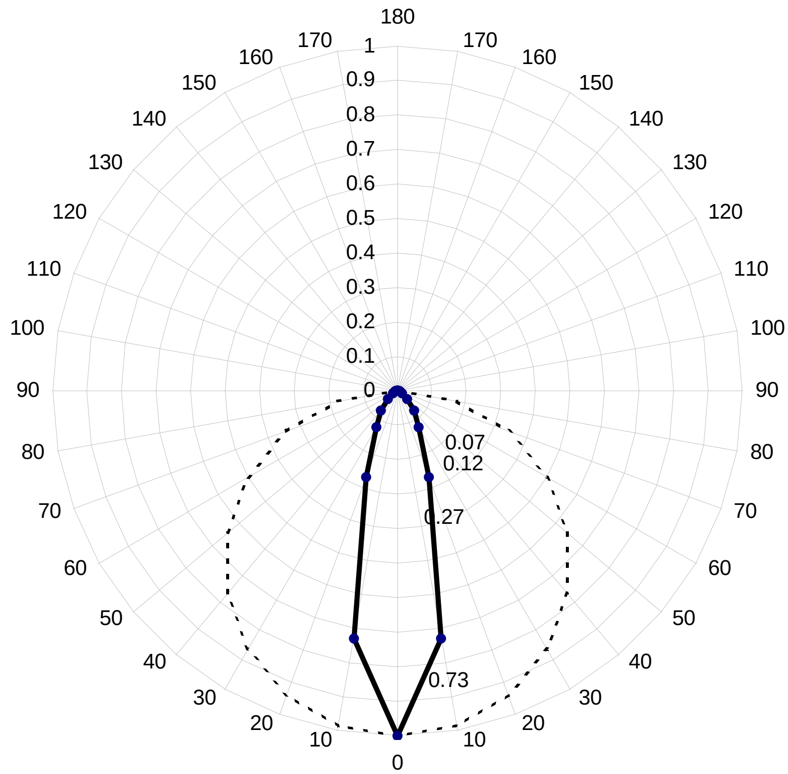

Recommendations

The spectral response function of the LS-201 photosensor is likely to be acceptable in many daylighting applications. Although its response curve is slightly narrower than the photopic curve, and the "peak" shifted slightly to the blue, it is better color-corrected than many of the photosensors currently on the market. One particularly favorable attribute is its insensivity to infrared radiation. Most photosensors available today for lighting control applications are based on silicon photodiodes which, if uncorrected, are more sensitive to the infrared portion of the electromagnetic spectrum than to visible light. Previous work has shown that photosensor sensitivity to IR can cause significant errors in control systems.

Because of the different physical principle underlying the operation of the LS-201, the sensor is entirely blind to IR. Essentially, photons with wavelengths greater than about 560 nm (for this LED) have insufficient energy to excite any charge carriers within the LED. Conversely, photons with shorter wavelengths than the peak response of the LED can excite charge carriers within the LED and this action tends to shift the "peak" of the spectral response function about 40 nm towards the blue. As a result, the sensor serves (fortuitously) as a decent *scotopic* meter. This has intriguing implications for the "Clear Vision" project that PG&E is investigating (see Emerging Technologies Coordinating Council database). Since a daylight control system built around the LS-201 would be more sensitive to the scotopic function than the photopic, the energy savings benefits of the scotopic research could be directly realized with an automatic control system assembled from hardware available today.

The spatial response function of the LS-201 as it currently stands is probably adequate for many applications. However, its narrow field of view (FOV), effectively a cone of 15 degree half-angle, may be overly sensitive to changes in the luminances in the FOV resulting in unexpected behavior of the lighting system under extreme conditions. Since the FOV for the sensor with the lens removed is significantly wider (a cone of 35 degree half-angle), it is the action of the lens itself that is causing the narrowing of the FOV. We would suggest replacing with the Fresnel lens with a slightly diffuse flat lens. This would judiciously broaden the FOV without compromising external appearance. A photosensor with a FOV of 35 degrees would not be sensitive to direct window light (which previous work indicates should be avoided) unless it were mounted very close to the window wall.

Overall, the LS-201 photosensor is the first commercially available control photosensor that we have seen that basically "gets it right." It implements the most appropriate control algorithm for daylighting ("sliding setpoint") as well as providing critical adjustments of gain, offset, and minimum trim. One cautionary note is that we have not run the simulations to ascertain that the correct range of commissioning adjustments have been realized in this product for daylit classroom applications. Furthermore, although all the correct commissioning adjustments are physically present, the sensor is a daunting array of trim pots and jumpers that can only be adjusted in the field by a person on a ladder. As it stands, the product could probably not pass the 5-minute commissioning test. However, it has been used successfully in recent building projects and *as long as sufficient time is* *allowed in the building contract for commissioning by a qualified commissioning agent*, the LS-201 may be an appropriate solution for many commercial daylighting applications.

Ideas for Future Development

With regards to product enhancement, it seems all the necessary adjustments have been realized in the physical circuit design using trim pots. Consequently, it should be straightforward to replace the trim pots with digital components (specifically 1-Wire digital potentiometers) of equivalent functionality. The use of 1-Wire devices in the photosensor provides network connectivity and allows the use of the 1-Wire communications protocol. This would allow the realization of a digitally-addressable photosensor that could be commissioned in the field remotely using a portable personal computer (PC) or even a PDA (i.e., PalmPilot). In order that such a sensor remain effective in the legacy analog world as well as the digital realm, we recommend that such a hybrid sensor be based on the IEEE P1451 Standard for Sensors and Actuators. The IEEE P1451 Standard provides a common format for digitally storing the sensor specifications (called the TEDS table) onboard the sensor itself. In addition, the Standard specifies the communications protocol for digitally transmitting sensor data onto a low-cost wired network. A sensor built to the IEEE P1451 Standard can continue to operate and add value to legacy analog equipment and still be ready for the emerging digitally-addressable lighting market.